Available online at www.sciencedirect.com
ScienceDirect
Journal of Organometallic Chemistry 693 (2008) 510–518
Journal of Organometallic Chemistry
www.elsevier.com/locate/jorganchem

Immobilization of a cationic ruthenium(II) complex containing the hemilabile phosphaallyl ligand in hexagonal mesoporous silica (HMS) and application of this material as hydrogenation catalyst

Dorota Duraczynska [a,*], Ewa M. Serwicka [a], Anna Waksmundzka-Gora [a], Alicja Drelinkiewicz [a], Zbigniew Olejniczak [b]

[a] *Institute of Catalysis and Surface Chemistry, Polish Academy of Sciences, ul. Niezapominajek 8, 30-239 Cracow, Poland*
[b] *Institute of Nuclear Physics, Polish Academy of Sciences, ul. Radzikowskiego 152, 31-342 Cracow, Poland*

Received 5 September 2007; received in revised form 16 November 2007; accepted 19 November 2007
Available online 23 November 2007

Abstract

The cationic ruthenium(II) complex $[(\eta^5\text{-}MeC_5H_4)Ru(\eta^3\text{-}PPh_2CHCH_2)(\eta^1\text{-}PPh_2CHCH_2)]^+$ (**1**) containing the hemilabile phosphaallyl ligand in two different coordination modes has been immobilized inside the pores of aluminated hexagonal mesoporous silica HMS(Si/Al = 40) by direct ion exchange method. This material was characterized by X-ray diffraction, thermogravimetric analysis, FTIR, solid state NMR (^{29}Si, ^{27}Al), UV–Vis, and X-ray photoelectron spectroscopies. The textural properties were determined from nitrogen adsorption at 77 K. (**1**)/HMS(Si/Al = 40) was shown to be active and selective in the catalytic hydrogenation of phenylacetylene.

Keywords: Hexagonal mesoporous silica HMS; Hydrogenation of phenylacetylene; Immobilization; Ion exchange method; Phosphaallyl ruthenium complex

1. Introduction

In spite of the superior performance of homogeneous catalysts over heterogeneous catalysts, the majority of large-scale industrial chemical processes employ heterogeneous catalysis. Homogeneous catalysts, frequently organometallic compounds, offer several advantages including the high selectivity, high activity, controllability as well as the detailed molecular insight. Unfortunately, the problems in separating them from the product(s), recovering and recycling, create demand for heterogeneous catalysts with comparable performance. The heterogenization of homogenous catalysts has been receiving much attention lately as a very convenient way of combining the advantages of the homogenous catalysts with those of heterogeneous catalysts. It may be accomplished by immobilization of transition metal complexes on suitable porous material, and can lead to a new class of systems whose catalytic properties are determined by both catalyst and host.

Various attempts toward the immobilization of ruthenium based catalysts have been undertaken previously such as encapsulation or encaging into porous material [1], grafting [2], tethering [3], metal dispersion [3], and immobilization in a liquid film formed on a support (SLPC) [4]. Ion exchange method, applicable to supports possessing exchange sites, seems to be the most useful since it enables the heterogenization of readily available ruthenium complexes and avoids the tedious and often very difficult task of ligand modification involved in many previously described methods.

The present study is focused on: (a) immobilization by means of ion exchange of the cationic ruthenium(II) complex $[(\eta^5\text{-}MeC_5H_4)Ru(\eta^3\text{-}PPh_2CHCH_2)(\eta^1\text{-}PPh_2CHCH_2)]^+$

* Corresponding author. Tel.: +48 126395142; fax: +48 124251923.
E-mail address: ncduracz@cyf-kr.edu.pl (D. Duraczynska).

0022-328X/$ - see front matter © 2007 Elsevier B.V. All rights reserved.
doi:10.1016/j.jorganchem.2007.11.032

(**1**) [5] containing hemilabile [6] ligand PPh_2CHCH_2 (diphenylvinylphosphine) onto porous HMS (hexagonal molecular sieve) [7] support possessing cation exchange properties due to partial alumination of the silica framework, (b) characterization of the resulting material, and (c) application of the supported cationic ruthenium(II) complex for the catalytic hydrogenation reaction of phenylacetylene. As shown on Scheme 1, the cationic ruthenium(II) complex $[(\eta^5\text{-}MeC_5H_4)Ru(\eta^3\text{-}PPh_2CHCH_2)(\eta^1\text{-}PPh_2CHCH_2)]^+$ (**1**) contains two different types of PPh_2CHCH_2 ligands bound to ruthenium center. One of these functionalities, $(\eta^3\text{-}PPh_2CHCH_2)$, is substitutionally labile and "opens" while used in catalytic reaction, providing a coordination site for an incoming substrate, and the other group, $(\eta^1\text{-}PPh_2CHCH_2)$, remains firmly bound to ruthenium center. The presence of such ligands in a complex may induce transformations that would not otherwise occur. Complexes of hemilabile ligands are of current interest because of their potential application in molecular activation, homogeneous catalysis, and small molecular sensing [8].

The discovery of mesoporous silica materials by the Mobil group [9] introduced new opportunities for designing organometallic complex/carrier systems and several reports on the immobilization of Ru based complexes onto MCM41-type mesoporous solids have appeared recently [10]. Although HMS materials also belong to the family of mesoporous silicas, they show important differences when compared to MCM-41 solids [7b]. In particular, they are characterized by a lower degree of long range ordering and a higher textural porosity. Pinnavaia and Tanev [7a] have indicated the importance of textural porosity in improving the transport of reagents in the mesostructure framework which makes HMS materials a better choice as a potential supports for the catalytically active phase. Mesoporous silicas can acquire cation exchange properties by partial substitution of Si^{4+} ions with Al^{3+} in the framework. It has been demonstrated that in HMS materials aluminated via direct procedure (Al source addition to the synthesis gel) cation exchange sites are localized preferentially on the inner pore walls [7f]. This feature ensures that an organometallic charge compensating cation becomes trapped inside the pore system. In our study the cationic ruthenium(II) complex $[(\eta^5\text{-}MeC_5H_4)Ru(\eta^3\text{-}PPh_2CHCH_2)(\eta^1\text{-}PPh_2CHCH_2)]^+$ (**1**) is ion exchanged onto aluminated HMS(Si/Al = 40) and bound to the carrier material by means of electrostatic interactions (Fig. 1).

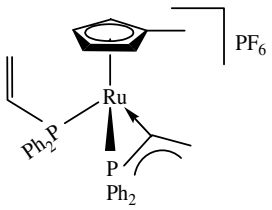

Scheme 1. Structure of the hexafluorophosphate salt of (**1**).

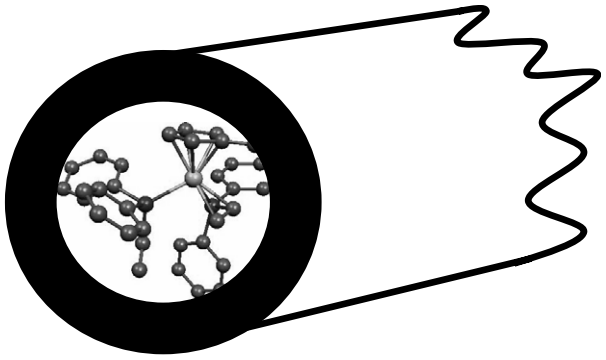

Fig. 1. Structural model of (**1**)/HMS(Si/Al = 40) catalyst.

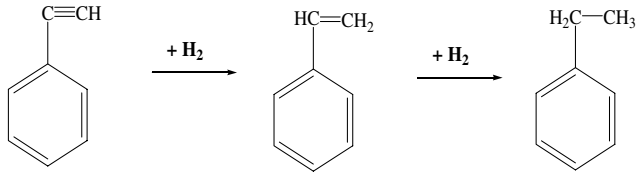

Scheme 2. Hydrogenation of phenylacetylene.

The catalytic reaction chosen in this work is the hydrogenation of phenylacetylene (Scheme 2) to styrene and ethylbenzene with dihydrogen gas in isopropanol solution. The selective hydrogenation of alkynes to alkenes has fundamental importance for the production of fine chemicals and industrial polymerization processes. Although there are a few examples of catalytically active homogeneous Ru–phosphines compounds in the hydrogenation of PhC≡CH (phenylacetylene) [11], there is very little information about the application of heterogeneous Ru–phosphine/carrier systems in this reaction.

2. Experimental

2.1. Materials

All chemicals used for the synthesis of the hexafluorophosphate salt of (**1**) were obtained from Sigma-Aldrich and used as purchased. The hexafluorophosphate salt of (**1**) was prepared according to the procedure published elsewhere [5]. Al, Si-mesoporous molecular sieves, referred to as HMS(Si/Al = 40) was obtained using the procedure described before [7]. The amounts of hexafluorophosphate salt of (**1**) and HMS(Si/Al = 40) in mechanical mixture are identical with those of supported catalyst.

2.2. Characterization procedures

UV–Vis absorbance spectra were recorded from CH_2Cl_2 solutions or Nujol thin film on a Shimadzu UV 160A spectrophotometer. The textural properties (surface area, pore volume) were determined from nitrogen adsorption at 77 K on AUTOSORB-1 (Qunata-Chrome) apparatus.

X-ray diffraction patterns were collected on a Siemens D5005 diffractometer using Cu Kα radiation. Fourier transform infrared (FTIR) spectra of the samples as KBr pellets were recorded on Nicolet 380 spectrophotometer. For thermogravimetric analysis a STA 409 PC Luxx (Netzsch) thermal analyzer was used. The heating rate was 10 °C/min, and α-Al_2O_3 was used as reference material. The X-ray Photoelectron Spectroscopy (XPS) measurements were performed in the ultrahigh vacuum (2×10^{-7} Pa) system equipped with hemispherical analyzer (SES R4000, Gammadata Scienta). The unmonochromatized Mg Kα X-ray source of incident energy of 1253.6 eV was applied to generate core excitation. The spectrometer was calibrated according to ISO 15472:2001. The energy resolution of the system in all experiments, measured as a full width at half maximum (FWHM) for Ag $3d_{5/2}$ excitation line, was 0.9 eV. The energy step at the survey spectra was 0.25 eV and the step at the detailed spectra was 0.025 eV. The spectra were calibrated for C 1s excitation at binding energy of 285.0 eV. The spectra were analyzed and processed with the use of CasaXPS 2.3.10. software. The background was approximated by Shirley algorithm and the detailed spectra were fitted with Voigt function. The accuracy of the XPS analysis is approximately 3%. High resolution, solid state Magic-Angle-Spinning Nuclear Magnetic Resonance (MAS NMR) spectra were measured on a Tecmag APOLLO pulse NMR spectrometer at the magnetic field of 7.05 T generated by the Magnex superconducting magnet. A Bruker HP-WB high-speed MAS probe equipped with the 4 mm zirconia rotor and KEL-F cap was used to record the MAS spectra at the spinning speeds ranging from 4 to 9 kHz. All NMR spectra were normalized to the same number of acquisitions and to the same mass of the sample. The solid state ^{29}Si MAS NMR spectra were measured at 59.517 MHz, using a single 3 μs radio-frequency (rf) pulse, corresponding to $\pi/2$ flipping angle. The spinning speed was 4 kHz. The acquisition delay used in accumulation was 60 s, and 256 scans were acquired. The frequency scale in ppm was referenced to the ^{29}Si resonance of tetramethylsilane (TMS). The solid state ^{27}Al MAS NMR spectra were measured at 78.066 MHz, using a single 2 μs rf pulse, corresponding to $\pi/6$ flipping angle. The spinning speed was 9 kHz. The acquisition delay used in accumulation was 1 s, and 2000 scans were acquired. The frequency scale in ppm was referenced to the ^{27}Al resonance of 1 M sample of $Al(NO_3)_3$. A gas chromatograph (Clarus 500, Perkin Elmer) with He as carrier gas (flow rate 1 ml/min) equipped with a capillary column Elite 5MS (0.25 μm × 0.25 mm × 30 m) and a flame ionization detector (FID) was used for analyzing the reaction mixture after catalysis. The identification of the hydrogenation products was achieved with a gas chromatograph coupled to a mass spectrometer (Perkin Elmer Auto System XL) equipped with PE-5MS column (0.25 μm × 0.25 mm × 30 m). The injector temperature was 200 °C and the heating rate 10 °C/min from 60 °C to 200 °C.

2.3. Immobilization of the cationic ruthenium(II) complex (1) onto HMS(Si/Al = 40)

The cationic ruthenium(II) complex (**1**) was incorporated into HMS(Si/Al = 40) by means of direct ion exchange method. A 100-ml, three-neck round bottom flask was charged with the hexafluorophosphate salt of (**1**) (0.075 g), methanol (40 ml), and the whole was heated under reflux. When all of the hexafluorophosphate salt of (**1**) had dissolved (yellow solution), HMS(Si/Al = 40) (0.9 g) as a white powder was added. The heterogeneous mixture was vigorously stirred at 55 °C for 24 h. The resulting yellow solid was separated by filtration and washed with warm methanol several times. After being dried in vacuum oven (70 °C), the supported catalyst was Soxhlet extracted with CH_2Cl_2 for 98 h in order to remove unreacted salt of (**1**). The amount of the adsorbed cationic ruthenium(II) complex (**1**) was determined by UV–Vis spectroscopy as a difference between quantity of (**1**) · PF_6 taken for the exchange and that remaining in the solution after filtering, washing and extraction. The content of (**1**) was estimated as 5.9 wt%.

2.4. Hydrogenation experiments

Hydrogenation experiments were carried out in an agitated batch glass reactor at constant atmospheric pressure of hydrogen (1 atm) with 2-propanol as the solvent. The following operating conditions were applied: temperature 40 °C, catalyst concentration 0.37 g/10 cm^3, initial phenylacetylene concentration (140×10^{-5} mol/dm^3). Before the hydrogenation experiment (in a typical procedure) the catalyst wetted with the solvent was activated in situ – inside the reactor by passing gaseous hydrogen through the reactor for 30 min, 15 min at 20 °C and 15 min at the temperature of reaction (40 °C in the standard procedure). Then, phenylacetylene solution was introduced and the hydrogenation reaction was started. Samples of liquids were withdrawn from the reactor via a sampling tube at appropriate intervals of time and they were analyzed by gas chromatography. The content of phenylacetylene, styrene and ethylbenzene formed in the hydrogenation was determined using standard compounds. At the end of a run the catalyst was separated by filtration.

3. Results and discussion

During the process of immobilization the surface reactivity of support can influence the geometry and electronic properties of metal in heterogenized organometallic compound. Moreover, the bonding character between metal and ligand(s) can be affected during the heterogenization process. We used many characterization techniques such as sorption studies, X-ray powder diffraction (XRD), thermogravimetric methods, Fourier transform infrared (FTIR) spectroscopy, X-ray photoelectron spectroscopy (XPS), UV–Vis spectroscopy, and solid-state NMR

spectroscopy in order to characterize the structures of organometallic ruthenium species and the carrier material HMS(Si/Al = 40) in heterogenized material. It was interesting to find out whether their structures remained intact or were changed upon immobilization process.

3.1. Sorption studies

Nitrogen adsorption isotherms of carrier material, HMS(Si/Al = 40), and of the support subjected to exchange with cationic ruthenium(II) complex, (**1**)/HMS(Si/Al = 40), are shown in Fig. 2. The data on the specific surface area and the pore volume are presented in Table 1. The DFT surface area was found to decrease from 647 m^2/g in the initial HMS(Si/Al = 40) to 407 m^2/g upon modification. Moreover the observed reduction in pore volume from 0.269 cm^3/g to 0.186 cm^3/g (Table 1) suggests that the cationic ruthenium(II) complex (**1**) is introduced inside the channels of the HMS(Si/Al = 40) support.

3.2. XRD

Fig. 3 shows the XRD patterns for the parent calcinated HMS(Si/Al = 40), the hexafluorophosphate salt of (**1**), mechanical mixture of hexafluorophosphate salt of (**1**) and the carrier material (**1**) · PF_6 + HMS(Si/Al = 40) (relative content as in the supported catalyst), and supported catalyst (**1**)/HMS(Si/Al = 40). The XRD diffraction pattern of the carrier material shows a very intense peak at $2\theta = 3°$ assigned to (1 0 0) reflection of the hexagonal mesostructure, and an additional broad, less intense signal within the 2θ region of 15–33° corresponding to amorphous silica. The XRD pattern for the physical mixture shows some peaks other than that of porous material HMS(Si/Al = 40), and they can be identified as those of the hexafluorophosphate salt of (**1**). On the other hand, the XRD pattern of supported catalyst is identical with that of parent material what proves that the structure of HMS(Si/Al = 40) is retained upon immobilization of (**1**).

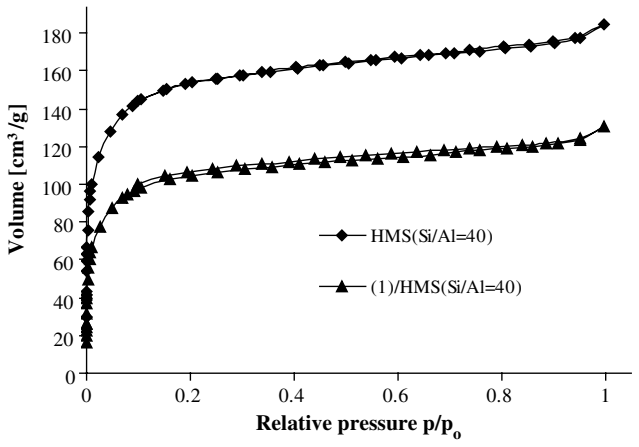

Fig. 2. N_2 adsorption/desorption isotherms of HMS(Si/Al = 40) and (**1**)/HMS(Si/Al = 40).

Table 1
Comparison of textural properties

Compound	Surface area[a] (m^2/g)	Pore volume[a] (cm^3/g)
HMS(Si/Al = 40)	647	0.269
(**1**)/HMS(Si/Al = 40)	407	0.186

[a] Calculated according to NLDFT Method.

3.3. Thermogravimetric studies

Thermogravimetric (TG) and differential thermogravimetric (DTG) analyses have been used to characterize thermal stability of ruthenium immobilized species (Fig. 4). Both analyzed samples, i.e. carrier material HMS(Si/Al = 40), and supported catalyst (**1**)/HMS(Si/Al = 40) show the weight loss at 80 °C that is attributed to the release of adsorbed water [7]. The further mass loss at 390 °C, observed only for HMS(Si/Al = 40) containing the immobilized cationic ruthenium(II) complex, is due to the decomposition and combustion of the organometallic component.

3.4. UV–Vis spectroscopy

The spectrum of the hexafluorophosphate salt of (**1**) dissolved in dichloromethane is dominated by a strong absorption with $\lambda_{max} = 233$ nm, presumably due to the intraligand π–π^* transitions (Fig. 5a) [12]. The sample obtained by cation exchange of hexafluorophosphate salt of (**1**) with HMS(Si/Al = 40) support shows a UV–Vis band with the same λ_{max}, which confirms that immobilization of the cationic ruthenium(II) complex (**1**) does occur (Fig. 5b). Small differences in the local environment of the deposited organometallic species are the most likely reason for the observed band broadening.

3.5. FTIR spectroscopy

Fourier transform IR spectra of the hexafluorophosphate salt of (**1**), carrier material HMS(Si/Al = 40), mechanical mixture of the hexafluorophosphate salt of (**1**) and the carrier material (**1**) · PF_6 + HMS(Si/Al = 40) (relative content as in the supported catalyst), and supported catalyst (**1**)/HMS(Si/Al = 40), are shown in Fig. 6. In the IR spectrum of the hexafluorophosphate salt of (**1**) a strong band at 840 cm^{-1} for ν(P–F) in PF_6^- counter-ion can clearly be seen. Although this band becomes very weak in the mechanical mixture it is still observed, thus showing that the structure of hexafluorophosphate salt of (**1**) is retained. On the other hand, this band completely disappears under immobilization procedure. This clearly proves that heterogenization of the hexafluorophosphate salt of (**1**) involves ion exchange mechanism, in which PF_6^- anions are left behind and only $[(\eta^5\text{-}MeC_5H_4)Ru(\eta^3\text{-}PPh_2CHCH_2)(\eta^1\text{-}PPh_2CHCH_2)]^+$ cations are retained by the support.

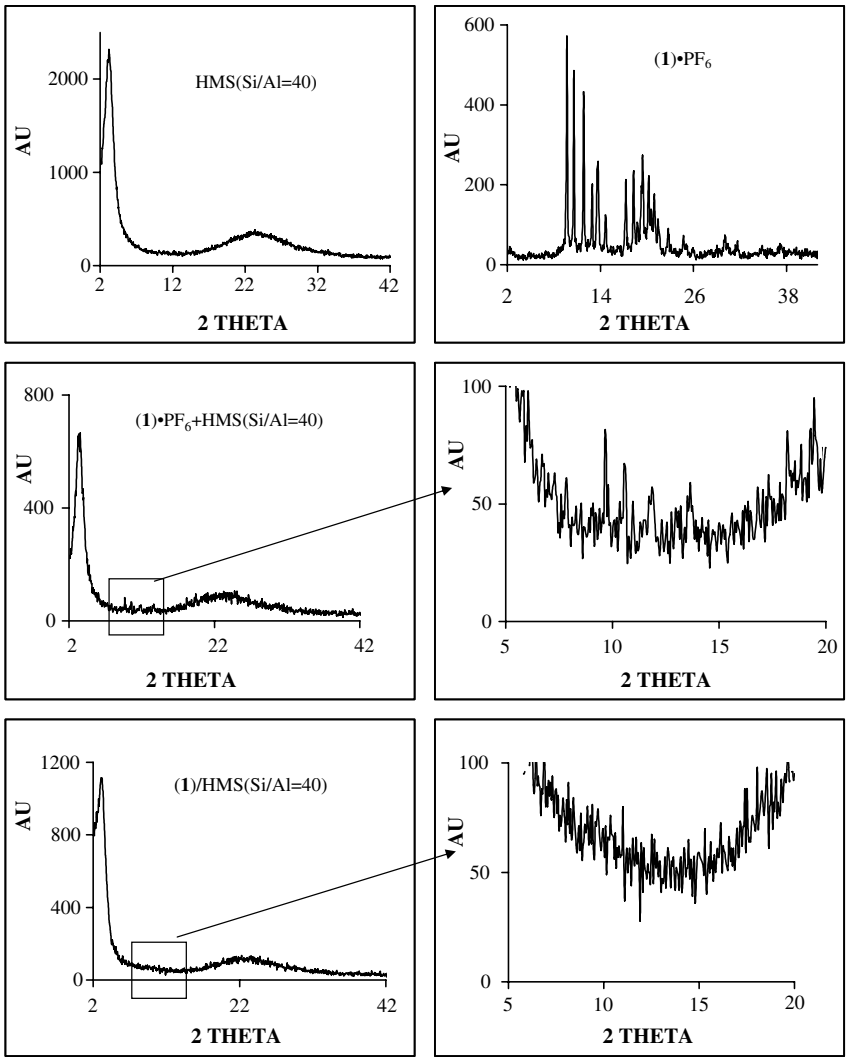

Fig. 3. XRD profiles of HMS(Si/Al = 40), (**1**) · PF_6, (**1**) · PF_6 + HMS(Si/Al = 40) and its expansion in the region between 5 and 20 2θ, (**1**)/HMS (Si/Al = 40) and its expansion in the region between 5 and 20 2θ.

3.6. X-ray photoelectron spectroscopy

There is very little information regarding reliable reference values of binding energies (BE) for ruthenium compounds [13]. Moreover the value of BE is very sensitive to changes in the nearest environment (e.g. types of ligands) and even commercially available Ru complexes are the mixtures of different species [13b]. In this work we studied Ru $3d_{5/2}$ level because of the overlapping of more intensive $3d_{3/2}$ level with the C 1s peak. The binding energies [eV] and the contributions [%] of the deconvoluted Ru $3d_{5/2}$ level components of the hexafluorophosphate salt of (**1**) and supported system (**1**)/HMS(Si/Al = 40) are presented in Table 2. The hexafluorophosphate salt of (**1**) exhibits three different Ru states at binding energies of 280.1 eV (12.3%), 281.7 eV (65.7%) and 283.4 eV (22%). In the case of supported catalyst two different Ru states are observed, major one at 281.7 (62.7%) and minor at 283.4 (37.3%) eV. These results indicate that the nature of ruthenium species do not change upon heterogenization since the values of BE of major components remain unchanged. The relative intensities of the component at 281.7 eV and that at 283.4 eV indicate that the former corresponds to the *exo* and the latter to the *endo* isomer of complex (**1**) · PF_6, whose content in the starting compound was determined by $^{31}P\{^1H\}$ NMR spectroscopy. The signal at 280.1 eV is most likely due to the presence of neutral $[(\eta^5\text{-}MeC_5H_4)_2Ru]$ in the starting material. The binding energies of analogous ruthenocenes $[(\eta^5\text{-}C_5H_5)_2Ru]$ and $[(\eta^5\text{-}Me_5C_5)_2Ru]$ were established as 280.7 eV and 279.0 eV, respectively [13a]. As expected, this neutral species does not undergo ionic exchange and is absent in the spectrum of immobilized complex.

3.7. NMR spectroscopy

In order to find out whether the structure of the carrier material HMS(Si/Al = 40) is affected by the immobilization, we recorded ^{29}Si- and ^{27}Al MAS NMR spectra (Figs. 7 and 8, respectively). The ^{29}Si spectrum of pure carrier

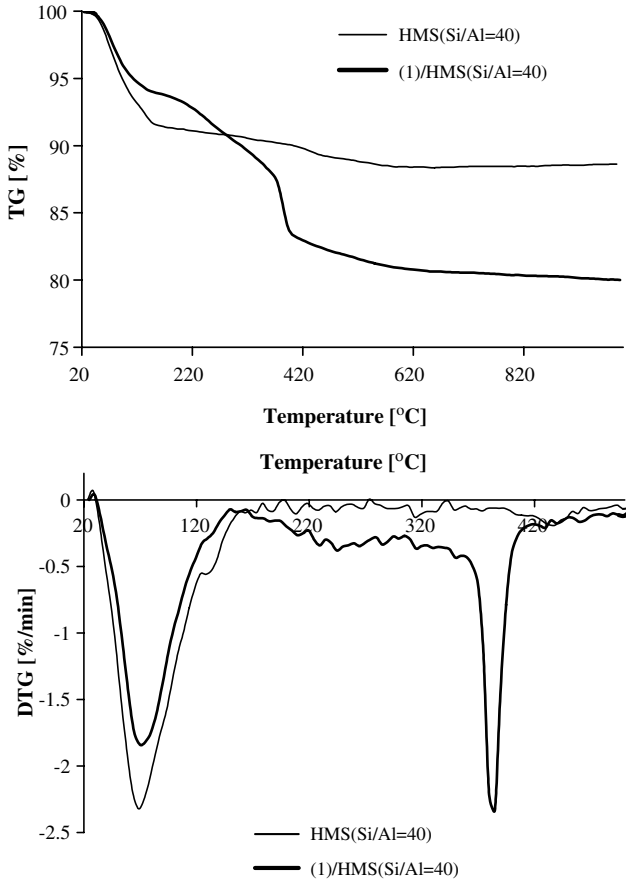

Fig. 4. Thermogravimetric analysis (TG) (top) and differential thermogravimetric analysis (DTG) (bottom) of HMS(Si/Al = 40), and (**1**)/HMS(Si/Al = 40).

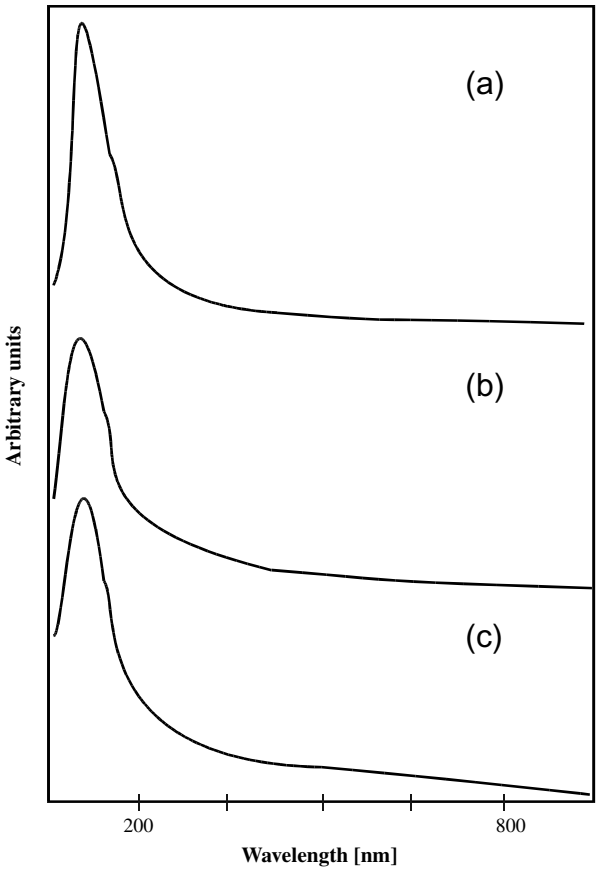

Fig. 5. The UV–Vis spectra of (a) (**1**) · PF_6 in CH_2Cl_2 solution, (b) (**1**)/HMS(Si/Al = 40) before catalysis, and (c) (**1**)/HMS(Si/Al = 40) after catalysis.

HMS(Si/Al = 40) shows an absorption whose major components appear at −110 ppm and −100 ppm (Fig. 7). The former can be attributed to Q_4 sites constituting of $Si(OSi)_4$ tetrahedra, the latter to Q_3 structural units of $Si(OSi)_3(OH)$ and $Si(OSi)_3(OAl)$ type [14]. Additionally, a slight downfield broadening of the spectrum points to a small contribution from resonance around −90 ppm, characteristic of Q_2 sites such as $Si(OSi)_2(OH)_2$, $Si(OSi)_2(OAl)_2$ and/or $Si(OSi)_2(OH)(OAl)$ units. The ^{29}Si spectrum of HMS(Si/Al = 40) containing the immobilized cationic ruthenium(II) complex is very similar to that of a pure support, the only minor difference consisting in a slightly larger relative contribution of the Q_3 line. This may be taken as an indication that, while essentially the bulk of the solid remains intact, a certain degree of hydrolysis of surface Si–O bonds occurs during the exchange carried out in the aqueous medium. ^{27}Al MAS NMR spectrum of the HMS(Si/Al = 40) material (Fig. 8) exhibits two resonance lines. Signal at 50 ppm can be assigned to tetrahedral aluminum species substituting for silicon in the mesoporous lattice. The peak at 0 ppm is due to extra framework six-coordinated aluminum sites. The narrow linewidth of this signal suggests that the responsible species possess some degree of rotational freedom, hence it is likely that the line is due chiefly to

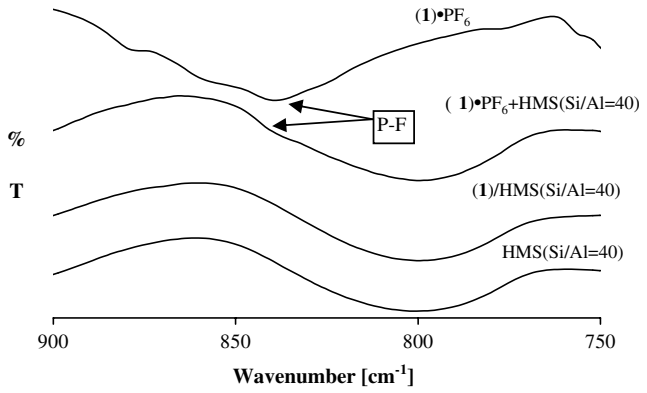

Fig. 6. FTIR spectra of (**1**) · PF_6, (**1**) · PF_6 + HMS(Si/Al = 40), (**1**)/HMS(Si/Al = 40) and HMS(Si/Al = 40) in 750-900 cm^{-1} region.

hydrated Al^{3+} cations. The spectrum of (**1**)/HMS(Si/Al = 40) sample shows that immobilization does not affect the signal of tetrahedral Al species, but the narrow signal at 0 ppm disappears. Apparently, the hydrated Al^{3+} complexes take part in cationic exchange and are removed from the sample during immobilization procedure. Indeed, in the sample subjected to cationic exchange the Si/Al ratio increases to 43. Additional confirmation comes from

Table 2
Binding energies (BE) and the contributions (%) of individual Ru $3d_{5/2}$ level components

Sample	BE (eV)	Contributions (%)
(**1**) · PF_6	280.1	12.3
	281.7	65.7
	283.4	22.0
(**1**)/HMS(Si/Al = 40)	281.7	62.7
	283.4	37.3

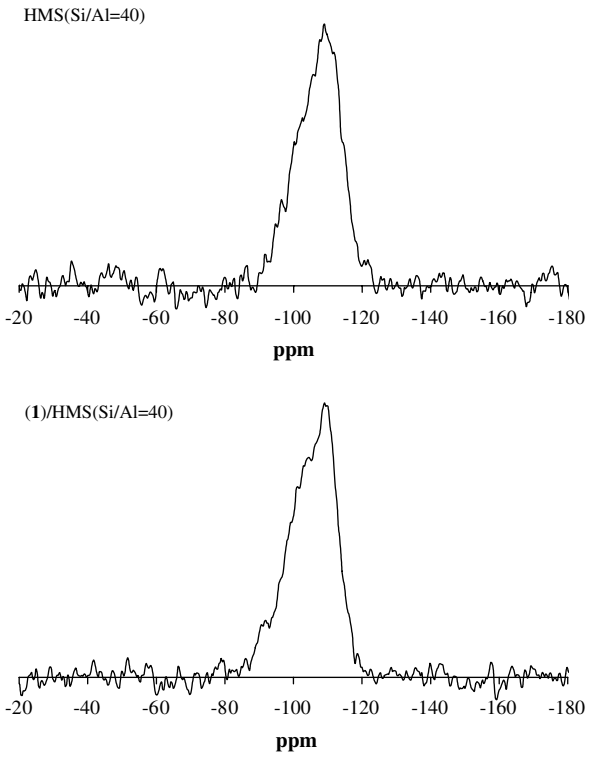

Fig. 7. ^{29}Si MAS NMR spectra of HMS(Si/Al = 40) (top), and (**1**)/HMS(Si/Al = 40) (bottom).

experiment in which the HMS(Si/Al = 40) support undergoes a similar treatment as during exchange procedure but in the solution free of hexafluorophosphate salt of (**1**). In the material treated this way the narrow signal at 0 ppm remains unchanged.

3.8. Catalytic activity

(**1**)/HMS(Si/Al = 40) was tested in the catalytic hydrogenation of phenylacetylene (Scheme 2). Literature data showed that phosphine–ruthenium complexes used in homogeneous systems were found to be catalytically active in this reaction [11]. For most complexes, this activity was observed under high pressure of hydrogen (30–80 atm) and/or high temperature (up to 90 °C), and/or required longer reaction time (15–24 h). Only two Ru–phosphine complexes, $[Ru(\eta^1\text{-}OCMe_2)(CO)_2(PPr^i_3)_2]BF_4$ [11e] and $[(PP_3)Ru(H)(H_2)]BPh_4$ [11f] (PP_3=$P(CH_2CH_2PPh_2)_3$) were active catalysts in the hydrogenation of phenylacetylene

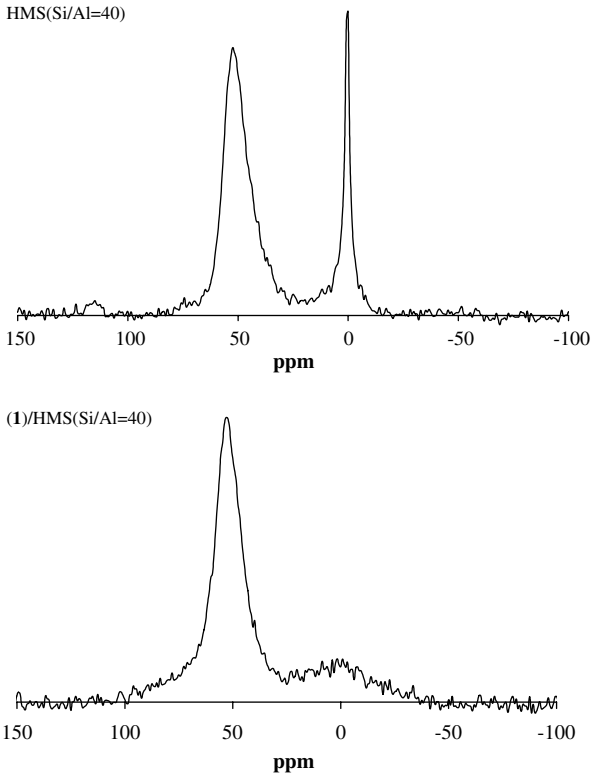

Fig. 8. ^{27}Al MAS NMR spectra of HMS(Si/Al = 40) (top), and (**1**)/HMS(Si/Al = 40) (bottom).

under mild conditions. However, in both cases the catalytic set up required the use of Schlenk line technique, in order to ensure oxygen-free and moisture-free atmosphere. The phosphaallyl complex (**1**) · PF_6 used in the present work is air-stable both in the solid state and in a solution.

The supported catalyst (**1**)/HMS(Si/Al = 40) containing 5.9 wt% of cationic ruthenium(II) complex (**1**) exhibited catalytic activity under mild condition: temperature 40 °C and H_2 pressure of 1 atm. GC–MS analysis showed that styrene and ethylbenzene were the only products formed in these conditions. The change of reagents content against reaction time in the presence of (**1**)/HMS(Si/Al = 40) is reported in Fig. 9. The major reaction pathway is the hydrogenation of the triple bond of phenylacetylene to yield styrene. The consecutive hydrogenation of styrene to ethylbenzene occurs as well, but due to its relatively low contribution, the selectivity to styrene as high as 86.5% is attained at 90% of phenylacetylene conversion. The activity of the supported catalyst, calculated as the initial rate of phenylacetylene conversion per 1 g of immobilized ruthenium species [$mol_{Phac}\, g^{-1}_{cat}\, min^{-1}$], is equal to 5.5×10^{-4}. Comparison of these values with the appropriate data for the hexafluorophosphate salt of (**1**) (Table 3) shows that the activity of the heterogenized system, is by 1/3 lower than that of the homogeneous catalyst. A possible explanation of this effect maybe a limited accessibility of some of the encapsulated cationic ruthenium(II) complexes, resulting in a lower turnover frequency of catalytic

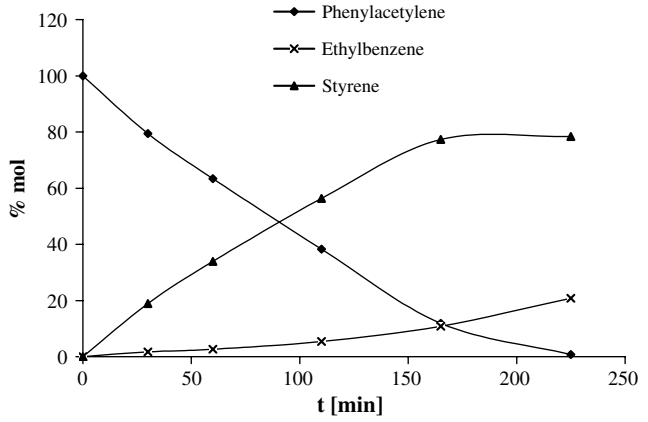

Fig. 9. Hydrogenation of phenylacetylene in the presence of 5.9 wt% (**1**)/HMS(Si/Al = 40).

Table 3
Catalytic activity (expressed as the initial rate of phenylacetylene conversion per 1 g of complex (**1**) · PF_6 and selectivity to styrene at 90% phenylacetylene conversion in the conditions of homogeneous and heterogeneous catalysis)

Catalyst	Activity rate of phenylacetylene hydrogenation ($mol_{Phac}\ min^{-1}\ g^{-1}_{com}$)	Selectivity to ST calculated at 90% phenylacetylene conversion (%)
(**1**) · PF_6 homogeneous	8.3×10^{-4}	86.9
(**1**)/HMS(Si/Al = 40) heterogeneous	5.5×10^{-4}	86.5

sites buried deep within the mesopore system. Immobilization has no adverse influence on the selectivity to styrene, which is equally high in both systems. Recent studies showed [15] that the decrease of catalytic activity of heterogenized catalysts compared to homogeneous catalysts is likely due to the change in the catalyst surface area available for the catalytic reaction. This possibility implies that the catalytically active zone is limited to the area near the pore mouth, where an efficient transport of substrates and products in and out of the pore may take place. In such a case for pores not differing significantly in size, the catalytic activity would depend primarily on the surface density of catalytic species. On the other hand, for the samples differing in the pore size the greater catalytic activity is observed for catalyst immobilized on supports with bigger pore sizes. The increased pore size allows for a larger fraction of the catalyst surface to participate in the catalytic reaction.

In order to check whether the reaction catalyzed by (**1**)/HMS(Si/Al = 40) is of truly heterogeneous nature, the reaction medium was analyzed for the presence of leached metal complex. The UV–Vis spectrum of solution separated from supported catalyst after the completion of hydrogenation showed no presence of absorption at $\lambda_{max} = 233$ nm, characteristic of the hexafluorophosphate salt of (**1**), thus proving that the immobilized ruthenium species remain anchored at the support. On the other hand, the UV–Vis spectra of the catalyst before and after hydrogenation reaction (see Figs. 5b and c, respectively) are identical, which shows that the immobilized cationic complex (**1**) not only stay bound to the carrier but also retain their electronic structure under the reaction conditions, a factor important from the point of view of a potential application.

Recently, Tschan et al. [11d] reported that a ruthenium dinuclear complex, when used as a homogeneous catalyst in the hydrogenation of phenylacetylene, underwent reaction with the substrate to give a new organometallic complex containing a styrenyl ligand. In view of the fact that earlier studies of the phosphaallyl $[(\eta^5\text{-}MeC_5H_4)Ru(\eta^3\text{-}PPh_2CH\text{-}CH_2)(\eta^1\text{-}PPh_2CHCH_2)]PF_6$ have shown that the compound may react with phenylacetylene to form a carbonyl compound $[(\eta^5\text{-}MeC_5H_4)Ru(PPh_2CHCH_2)_2(CO)]PF_6$ [5], we have decided to check whether such a complex was formed in the conditions of homogeneous hydrogenation of phenylacetylene. For this purpose the homogeneous catalyst was recovered after the reaction and subjected to IR analysis. Its spectrum was identical with that of complex $[(\eta^5\text{-}MeC_5H_4)Ru(\eta^3\text{-}PPh_2CHCH_2)(\eta^1\text{-}PPh_2CHCH_2)]PF_6$. In particular, no band at 1983 cm^{-1}, characteristic for ν_{CO} of the carbonyl compound [5], appeared in the recovered material, which excludes the formation of carbonyl complex during catalytic reaction.

We would like to emphasize that the catalytic data presented in this paper are preliminary and the reaction conditions are not optimized. The experiments are under progress to find the correlation between the loading of catalytic active ruthenium species and catalytic activity of (**1**)/carrier system in the phenylacetylene hydrogenation.

4. Conclusions

Heterogenized catalyst was obtained by immobilization of cationic ruthenium(II) complex $[(\eta^5\text{-}MeC_5H_4)Ru(\eta^3\text{-}PPh_2CHCH_2)(\eta^1\text{-}PPh_2CHCH_2)]^+$ (**1**) onto aluminated hexagonal mesoporous silica HMS(Si/Al = 40) by direct ion exchange method. Physicochemical characterization confirms that the ruthenium(II) cations are trapped by the support, and that the immobilized complex retains its essential characteristics. The catalytic test of phenylacetylene hydrogenation shows that the activity of the supported catalyst represents ca. 2/3 of that observed for the homogeneous catalyst, with the selectivity to styrene remaining at the same, very high level (87% at 90% phenylacetylene conversion). The lower activity of supported catalyst compared to that of the hexafluorophosphate salt of (**1**) is tentatively assigned to limited accessibility of some of the active ruthenium(II) sites localized within the mesopore system. Supported catalyst (**1**)/HMS(Si/Al = 40) is stable under catalytic conditions and shows no leaching into the reaction medium, which renders the material ready for recycling and reuse.

Acknowledgements

D.D. acknowledges the financial support from the European Commission within the "Transfer of Knowledge in Design of Porous Catalysts" TOK-CATA programme (research project MTKD-CT-2004-509832) and POL-POST DOC II (project D037/H03/2006). We thank Dr. J. Gurgul and Dr. R. Socha from Institute of Catalysis and Surface Chemistry PAS for the XPS analysis. The authors are grateful to Prof. T. Szymanska-Buzar and Dr. B. Biernat from the Chemistry Department of University of Wroclaw for the help with photochemical reactions while preparing complex (**1**) · PF_6.

References

[1] (a) T. Joseph, D.P. Sawant, C.S. Gopinath, S.B. Halligudi, J. Mol. Catal. A: Chem. 184 (2002) 289–299;
(b) J.R. Kincaid, Chem. Eur. J. 6 (2000) 4055–4061;
(c) E. Briot, F. Bedioui, K.J. Balkus Jr., J. Electroanal. Chem. 454 (1998) 83–89;
(d) G.-C. Shen, A.M. Liu, M. Ichikawa, Inorg. Chem. 37 (1998) 5497–5506;
(e) A.A. Bhuiyan, J.R. Kincaid, Inorg. Chem. 37 (1998) 2525–2530.

[2] (a) K. Fujishima, A. Fukuoka, A. Yamagishi, S. Inagaki, Y. Fukushima, M. Ichikawa, J. Mol. Catal. A: Chem. 166 (2001) 211–218;
(b) V. Huc, M. Saveyroux, J.P. Bourgoin, F. Valin, G. Zalczer, P.A. Albouy, S. Palacin, Langmuir 16 (2000) 1770–1776;
(c) K. Motokura, T. Mizugaki, K. Ebitani, K. Kaneda, Tetrahedron Lett. 45 (2004) 6029–6032;
(d) C.M. Standfest-Hauser, T. Lummerstorfer, R. Schmid, K. Kirchner, H. Hoffmann, M. Puchberger, Monatsh. Chem. 134 (2003) 1167–1175;
(e) B. Cetinkaya, N. Gurbuz, T. Seckin, I. Ozdemir, J. Mol. Catal. A: Chem. 184 (2002) 31–38.

[3] (a) C. Bianchini, V. Dal Santo, A. Meli, S. Moneti, M. Moreno, W. Oberhauser, R. Psaro, L. Sordelli, F. Vizza, J. Catal. 213 (2003) 47–62;
(b) K. Melis, D. De Vos, P. Jacobs, F. Verpoort, J. Mol. Catal. A: Chem. 169 (2001) 47–56.

[4] (a) W. Strohmeier, B. Graser, R. Mercec, K. Holke, J. Mol. Catal. 11 (1981) 257–262;
(b) S.-I. Fujita, Y. Sano, B.M. Bhanage, M. Arai, J. Catal. 225 (2004) 95–104;
(c) J. Horniakova, H. Nakamura, R. Kawase, K. Komura, Y. Kubota, Y. Sugi, J. Mol. Catal. A: Chem. 233 (2005) 49–54.

[5] D. Duraczyńska, J.H. Nelson, Dalton Trans. (2003) 449–457.

[6] (a) J.C. Jeffrey, T.B. Rauchfuss, Inorg. Chem. 18 (1979) 2658–2666;
(b) M. Martin, O. Gevert, H. Werner, J. Chem. Soc. Dalton Trans. (1996) 2275–2283, and references therein;
(c) H. Werner, A. Stark, M. Schulz, J. Wolf, Organometallics 11 (1992) 1126–1130;
(d) M.A. Esteruelas, A.M. Lopez, L.A. Oro, A. Perez, M. Schulz, H. Werner, Organometallics 12 (1993) 1823–1830;
(e) M.R. Mason, J.G. Verkade, Organometallics 11 (1992) 1514–1520;
(f) C.A. Sassano, C.A. Mirkin, J. Am. Chem. Soc. 117 (1995) 11379–11380;
(g) E. Lindner, M. Haustein, R. Fawzi, M. Steimann, P. Wegner, Organometallics 13 (1994) 5021–5029;
(h) T. Braun, P. Steinert, H. Werner, J. Organomet. Chem. 488 (1995) 169–176;
(i) G.W. Parshall, S.D. Ittel, Homogeneous Catalysis: The Applications and Chemistry of Catalysis by Soluble Transition Metal Complexes, second ed., Wiley-Interscience, New York, 1992, pp. 70–72;
(j) W. Keim, Angew. Chem. Int. Ed. Engl. 29 (1990) 235–244;
(k) J. Andrieu, P. Braunstein, F. Naud, R.D. Adams, R. Layland, Bull. Soc. Chem. Fr. 133 (1996) 669–672;
(l) P. Braunstein, F. Naud, Angew. Chem. Int. Ed. 40 (2001) 680–699.

[7] (a) P.T. Tanev, T.J. Pinnavaia, Science 267 (1995) 865–867;
(b) P.T. Tanev, T.J. Pinnavaia, Chem. Mater. 8 (1996) 2068–2079;
(c) H.-Y. Lin, Y.-W. Chen, J. Porous Mater. 12 (2005) 95–105;
(d) J. Poltowicz, E.M. Serwicka, E. Bastardo-Gonzalez, W. Jones, R. Mokaya, Appl. Catal. A: General 218 (2001) 211–217;
(e) R. Mokaya, W. Jones, Chem. Commun. (1996) 981–982;
(f) E.M. Serwicka, R. Mokaya, J. Poltowicz, W. Jones, ChemPhysChem 3 (2002) 892–896.

[8] S.E. Angell, C.W. Rogers, Y. Zhang, M.O. Wolf, W.E. Jones Jr., Coord. Chem. Rev. 250 (2006) 1829–1841, and references therein.

[9] J.S. Beck, J.C. Vartuli, W.J. Roth, M.E. Leonowicz, C.T. Kresge, K.D. Schmitt, C.T.-W. Chu, D.H. Olson, E.W. Sheppard, S.B. McCullen, J.B. Higgins, J.L. Schlenker, J. Am. Chem. Soc. 114 (1992) 10834–10843.

[10] (a) T. Joseph, S.S. Deshpande, S.B. Halligudi, A. Vinu, S. Ernst, M. Hartmann, J. Mol. Catal. A: Chem. 206 (2003) 13–21;
(b) P. Stepnicka, J. Demel, J. Cejka, J. Mol. Catal. A: Chem. 224 (2004) 161–169.

[11] (a) B. Punji, J.T. Mague, M.S. Balakrishna, J. Organomet. Chem. 691 (2006) 4265–4272;
(b) A. Caballero, F.A. Jalon, B.R. Manzano, G. Espino, M. Perez-Manrique, A. Mucientes, F.J. Poblete, M. Maestro, Organometallics 23 (2004) 5694–5706;
(c) I. Moldes, E. de la Encarnacion, J. Ros, A. Alvarez-Larena, J.F. Piniella, J. Organomet. Chem. 566 (1998) 165–174;
(d) M.J.-L. Tschan, G. Suss-Fink, F. Cherioux, B. Therrien, Chem. Eur. J. 13 (2007) 292–299;
(e) R. Atencio, C. Bohanna, M.A. Esteruelas, F.J. Lahoz, L.A. Oro, J. Chem. Soc. Dalton Trans. (1995) 2171–2181;
(f) C. Bianchini, C. Bohanna, M.A. Esteruelas, P. Frediani, A. Meli, L.A. Oro, M. Peruzzini, Organometallics 11 (1992) 3837–3844.

[12] G. Venkatachalam, R. Ramesh, S.M. Mobin, J. Organomet. Chem. 690 (2005) 3937–3945.

[13] (a) P.G. Gassman, C.H. Winter, J. Am. Chem. Soc. 110 (1988) 6130–6135;
(b) P. Froment, M.J. Genet, M. Devillers, J. Electron. Spectrosc. Relat. Phenom. 104 (1999) 119–126;
(c) M. van Veenendaal, Phys. Rev. B. 74 (2006) 085118-1–085118-6;
(d) C.L. Bianchi, V. Ragaini, M.G. Cattania, Mater. Chem. Phys. 29 (1991) 297–306;
(e) U.S. National Institute of Standards and Technology (NIST) XPS database http://srdata.nist.gov/xps and references therein.

[14] W. Kolodziejski, A. Corma, M.T. Navarro, J. Perez-Pariente, Solid State Nucl. Magn. Reson. 2 (1993) 253–259.

[15] L. Matachowski, K. Pamin, J. Poltowicz, E.M. Serwicka, W. Jones, R. Mokaya, Appl. Catal. A: General 313 (2006) 106–111.